

AD-A009 769

FREQUENCY RESPONSE OF THE OCULOVESTIBULAR SYSTEM  
DURING YAW OSCILLATION

W. Carroll Hixson

Naval Aerospace Medical Research Laboratory  
Pensacola, Florida

8 December 1974

DISTRIBUTED BY:

**NTIS**

National Technical Information Service  
U. S. DEPARTMENT OF COMMERCE

UNCLASSIFIED

Security Classification

AD-A009 769

## DOCUMENT CONTROL DATA - R &amp; D

(Security classification of title, body of abstract and indexing annotation must be entered when the overall report is classified)

1. ORIGINATING ACTIVITY (Corporate author) Naval Aerospace Medical Research Laboratory Pensacola, Florida 32512		2a. REPORT SECURITY CLASSIFICATION Unclassified	
		2b. GROUP N/A	
3. REPORT TITLE FREQUENCY RESPONSE OF THE OCULOVESTIBULAR SYSTEM DURING YAW OSCILLATION			
4. DESCRIPTIVE NOTES (Type of report and inclusive dates)			
5. AUTHOR(S) (First name, middle initial, last name) W. Carroll Hixson			
6. REPORT DATE 8 December 1974		7a. TOTAL NO. OF PAGES 31	7b. NO. OF REFS 15
8a. CONTRACT OR GRANT NO.		8b. ORIGINATOR'S REPORT NUMBER(S) NAMRL-1212	
b. PROJECT NO. MF51.524.005-7016 DE1G		9b. OTHER REPORT NO(S) (Any other numbers that may be assigned this report)	
c.			
d.			
10. DISTRIBUTION STATEMENT Approved for public release; distribution unlimited.			
11. SUPPLEMENTARY NOTES		12. SPONSORING MILITARY ACTIVITY	
13. ABSTRACT The report describes the results of a system transfer function type study of the oculovestibular response to sinusoidal yaw angular oscillations of the head. Ten naval aviator candidates were exposed to Earth-vertical rotation about the z head axis at nine different, octave-separated stimulus frequencies covering the 0.005 to 1.28 Hz spectrum with peak velocity of the stimulus held constant at 50 deg/sec. The frequency dependence of the oculovestibular system was interpreted in terms of phase and amplitude measures of the slow component eye velocity element of the resulting horizontal nystagmus. Though the phase data collected at the lower stimulus frequencies deviated somewhat from those predicted by the conventional second-order model of cupula-endolymph response, a theoretical account for the deviation was postulated by introducing an adaptation transfer function as developed by other investigators. An adaptation time constant of 100 sec was found to best fit the raw phase data, using two different phase selection criteria. With this modification of the raw phase data, it was predicted that the lower corner frequency of the cupula-endolymph system is approximately 0.0085 Hz (a long time constant of 19 sec). Brief discussion is presented of an unexplained peak in nystagmus beat frequency at 0.16 Hz and apparent conflicts in the amplitude data at the higher stimulus frequencies.			

Reproduced by  
NATIONAL TECHNICAL  
INFORMATION SERVICE  
US Department of Commerce  
Springfield, VA. 22151

DD FORM 1473 (PAGE 0)  
1 NOV 65  
S/N 0101-807-6801

PRICES SUBJECT TO CHANGE  
UNCLASSIFIED  
Security Classification

UNCLASSIFIED

Security Classification

14. KEY WORDS	LINK A		LINK B		LINK C	
	ROLE	WT	ROLE	WT	ROLE	WT
Aerospace medicine						
Human effectiveness						
Flight forces						
Angular acceleration						
Labyrinth						
Oculovestibular system						
Semicircular canals						
Cupula-endolymph mechanism						
Eye motions						
Nystagmus						
Biological models						
Frequency response						
System transfer functions						
Bioengineering						

Approved for public release; distribution unlimited

FREQUENCY RESPONSE OF THE OCULOVESTIBULAR SYSTEM  
DURING YAW OSCILLATION

W. Carroll Hixson

Bureau of Medicine and Surgery  
MF51.524.005-7016 DEIG

Approved by

Ashton Graybiel, M.D.  
Assistant for Scientific Programs

Released by

Captain N. W. Allebach, MC, USN  
Officer in Charge

8 December 1974

NAVAL AEROSPACE MEDICAL RESEARCH LABORATORY  
PENSACOLA, FLORIDA 32512

*ik*

## SUMMARY PAGE

### THE PROBLEM

The need to develop mathematical descriptors and models of vestibular function in a format suitable for bioengineering-type analyses of the effects of unusual military motion environments on crew performance.

### FINDINGS

A determination was made of the oculovestibular response of ten naval aviator candidates exposed to nine different, octave-separated yaw oscillation frequencies covering the 0.005 to 1.28 Hz spectrum. The frequency dependence of the system was interpreted in terms of phase and amplitude measures of the resulting horizontal nystagmus evoked at each stimulus frequency. The phase data at the lower stimulus frequencies were observed to deviate considerably from those predicted by conventional second-order descriptions of canal function. However, a theoretical account for these deviations was provided by introducing an adaptation transfer function as proposed by other investigators. An adaptation time-constant of 100 sec was found to best represent the phase response. The resulting modified phase data predict a lower corner-frequency of 0.0085 Hz (a long time-constant of 19 sec) for the cupula-endolymph system.

### ACKNOWLEDGMENTS

The author wishes to express his appreciation to Mr. A. N. Dennis, Jr., for the sincere interest he devoted to the conduct of the experiment.

In addition, reluctant congratulations are extended to Jorma I. Niven, the author's long-term co-investigator, for his decision to enjoy the retirement life. Simply said, it was the author's privilege to have participated with this investigator in many personally rewarding research experiences over the past 20 years.

## INTRODUCTION

The difficulties associated with the exposure of man's vestibular system to the complex flight-force environment defined by tactical operations of military aircraft have been long recognized to define a most significant problem area in aerospace medicine. The end result of these difficulties, whether manifested in the form of disorientation, vertigo, motion sickness, or vision modification, is degradation of crew performance. Furthermore, as new design concepts for aircraft and related weapons systems are developed and released for operational application, the problem becomes even more complex. For example, the high-performance flight characteristics of the F-14 Tom Cat create new tolerance level requirements for g stress; the VTOL capabilities of the AV-8A Harrier present a difficult spatial orientation task during the transitions to and from vertical flight; and the potential development of new aircraft types, or modification of existing types, to provide the pilot with vectored aerodynamic thrust in one or two dimensions while performing tactical maneuvers will further stress the orientation task. Relative to weapon systems, the recent in-combat demonstration of highly effective ground-to-air missiles has placed new demands on a wide variety of military aircraft as a result of the tactical need to develop effective, high-stress, missile avoidance maneuvers.

It should be recognized also that the potential for vestibular-related performance degradation is not at all confined to only the military flight environment. Current developments in military surface effects ships indicate that the high-level, low-frequency motion stimuli produced by these vessels may evoke pronounced vestibular reactions. Vestibular difficulties are also experienced in the military underseas environment involving free-swimming divers working at great depths or under poor illumination conditions. It is to be expected that these difficulties will become further complicated as diving technology develops and extends present-day depth limits.

Though these military environments differ considerably in terms of their physical characteristics, all have the common requirement for baseline biological data that can better define the over-all vestibular effect of the motion stimuli on crew performance. For example, from the vehicle design viewpoint there is a requirement for

engineering-oriented mathematical models of vestibular performance that can quantitatively link the force characteristics of a given motion environment to the magnitude and form of the vestibular responses that will be elicited. With this form of information, vehicle design alternatives can be better evaluated so as to select motion characteristics, instrument features, display media, or crew postures that optimize performance of the vehicle-crew combination. Similar requirements arise in the design and development of motion-based simulators to train crew personnel to operate a given vehicle or weapons system. For this situation, baseline vestibular data are required to ensure the selection of simulator motion characteristics that maximize the positive transfer of training experience to the operational situation. The selection of individuals to receive formal crew training involves corresponding requirements in that normative data are required to screen and select those individuals with minimal susceptibility to the given motion environment.

The present investigation is addressed primarily toward the engineering-related problem areas just discussed in that it is the long-term objective to develop mathematical descriptors and models of vestibular response that can be directly linked to specific linear and angular acceleration components of the motion environment. It is fully recognized that the development of these descriptors and models is a formidable long-term task for researchers in the vestibular field in that the dual-triaxial sensing mechanisms of the labyrinth respond differently when these accelerations act in combination rather than singly with many interactions existing within and external to these mechanisms. The specific objective of this study is to approach the problem in building-block form by presenting data which describe the frequency-response characteristics of the oculovestibular system during yaw angular oscillation. Phase and amplitude measures of the horizontal nystagmus produced at nine different, octave-separated stimulus frequencies were recorded and analyzed for ten naval aviator candidates. As with previous work in this area (refs. 11 and 8), interpretation of the results is keyed to the system transfer function representation (refs. 7 and 12) of vestibular performance.

## PROCEDURE

The variable-frequency sinusoidal angular acceleration stimuli used in the experiment were generated by the Periodic Angular Rotator (PAR), a single-axis rotating device developed for investigation of the dynamic response characteristics of the oculovestibular system (ref. 9). The rotating element of the device is a bearing-supported chair that is free to turn in either direction about an Earth-vertical axis. Motive power is provided by a gearless DC torque motor that is direct-coupled to the base of the subject chair. The system is operated as a closed-loop power servomechanism that may be controlled in either a velocity or displacement mode. Velocity feedback is provided by a small DC torque tachometer that is in-line coupled to the lower shaft of the main drive motor. Displacement feedback is obtained from a single turn, infinite resolution potentiometer that is also in-line coupled to the drive system. For this experiment, PAR was operated in the velocity mode with command provided by an RC type low-frequency oscillator (Krohn-Hite Model 4024) with sinusoidal output. This type of oscillator was selected in lieu of a conventional synthesized waveform function generator to eliminate the staircase acceleration steps produced by the latter.

As indicated in Table I, each subject was exposed to nine different stimulus frequencies covering an eight-octave spectrum ranging from 0.005 to 1.28 Hz. During this sinusoidal stimulation, the head was located on the rotational center of the device and oriented so that the z (head-foot) axis was in alignment with the rotational axis. Throughout the experiment the peak angular velocity of each sinusoidal stimulus was maintained constant at 50 deg/sec. To minimize the effects of fatigue or long-term adaptation, four different testing sessions, identified as A, B, C, and D, were used to present the nine stimulus frequencies. Because of the considerable length of the cyclic periods associated with the 0.005 and 0.01 Hz stimuli, a separate testing session was allotted to each of these frequencies.

The instantaneous amplitude of the nystagmic displacements of the eye in the horizontal direction, i.e., yaw rotation of the eye about the z axis, was recorded throughout each stimulus period. Of direct concern to the experiment was the peak velocity of the slow component of nystagmus that occurred during each cyclic half-period, and the phase difference between the reversals in direction of nystagmus slow-component velocity and the reversals in direction of the angular acceleration stimulus.



**TABLE I**  
**Characteristics of Sinusoidal Angular Acceleration Stimuli: Rotation about the z head axis**

Stimulus Parameter	Experimental Condition								
Testing Session Code Letter	A	B	C	C	C	D	D	D	D
Stimulus Code Number	1	2	3	4	5	6	7	8	9
Cyclic Frequency (Hertz)	0.005	0.01	0.02	0.04	0.08	0.16	0.32	0.64	1.28
Angular Frequency (rad/sec)	0.31	0.063	0.13	0.25	0.50	1.00	2.01	4.02	8.04
Cyclic Period (seconds)	200	100	50	25	12.5	6.25	3.12	1.56	0.78
Peak Angular Displacement (deg)	1592	796	398	199	99	49.7	24.9	12.4	6.2
Peak Angular Velocity (deg/sec)	50	50	50	50	50	50	50	50	50
Peak Angular Acceleration (deg/sec <sup>2</sup> )	1.57	3.14	6.28	12.6	25.1	50.2	100	201	402
Number of Response Transitions Scored per Stimulus Condition	4	4	4	8	16	20	20	20	20

DC recordings of eye displacement were made using conventional corneoretinal potential technique. The displacement signal, derived from silver chloride electrodes placed at the outer canthi of each eye, was amplified by a direct-coupled, differential-input preamplifier with adjustable zero suppression (Hewlett-Packard Model 350-1500 amplifier and Model 350-2 coupler) and displayed on a direct-writing recorder. The preamplifier filtering circuitry was adjusted to produce an over-all frequency response extending from DC to an upper corner frequency of 30 Hz.

An ancillary instrumentation requirement of this experiment was to establish a measurement reference for the nystagmus phase data that would precisely define each reversal in stimulus direction. Of primary concern was the possibility that the system tachometer normally used to establish stimulus transitions would introduce phase errors at the higher stimulus frequencies. To evaluate this possibility, two force-

balance type servo accelerometers were installed on the PAR device as follows: One transducer, a  $\pm 5g$  linear accelerometer with a natural frequency of 190 Hz and a damping ratio of 0.7 (Donner Model 4310), was mounted radially approximately 3 feet from the rotational center of PAR. The second transducer, a  $\pm 10$  rad/sec angular accelerometer with a natural frequency of 104 Hz and a damping ratio of 0.7 (Donner Model 4525), was mounted on the rotational center of the device. The system, including a seated subject, was then oscillated at each of the higher stimulus frequencies and simultaneous recordings made of the tachometer output voltage, the displacement potentiometer output voltage, the radial linear accelerometer output representing device centripetal acceleration, and the angular accelerometer output representing device angular acceleration. Since the resulting data indicated that the tachometer signal was in slight phase error at the higher stimulus frequencies, the displacement transducer signal was used as timing reference for measurement of nystagmus phase lag. These data also indicated that at an oscillation frequency of 2.56 Hz (the next octave above the upper frequency used in the experiment), amplitude distortion was present in the angular acceleration waveform even though distortion was not readily apparent in the tachometer velocity signal. For this reason, the upper frequency limit for the study was restricted to 1.28 Hz.

The subjects were volunteer, male, student naval aviators, all in apparent good health and with no known defects of hearing or equilibrium. Instruction was given to each of them regarding the purpose of the experiment, the nystagmus recording procedure, and the nature of the rotational stimuli he would experience. Each was then given an indoctrination ride in the PAR device and exposed to two of the stimulus frequencies; the first was one of the three frequencies in the C session, the second was always the 0.005 Hz frequency associated with the A session. The indoctrination run served to familiarize each subject with the relatively mild nature of the device oscillations. Equally important, the nystagmus data also served a basic screening function. If a readable nystagmus record was produced in response to the low-level 0.005 Hz stimulus, the subject was accepted as a member of the test group. Of a total of 23 subjects exposed to the indoctrination run, ten were rejected because of either noise artifacts produced by muscle tremor, widespread amplitude variations, or low response

at 0.005 Hz. Of the thirteen subjects who satisfied the screening criteria, one was used to collect pilot data and two were forced to withdraw midway during the experiment due to scheduling difficulties.

Upon completion of the screening phase, each selected subject was assigned a schedule for the four testing sessions outlined in Table 1. This schedule was arranged so that each subject was limited to a maximum of two testing sessions per day with the condition that a minimum resting period of at least 4 hours exists between sessions. In practice, however, most subjects were exposed to only one testing session per day. For each session the subject was instrumented with nystagmus electrodes approximately 30 minutes before presentation of the first stimulus. During this waiting period, the subject was exposed to subdued lighting in the interest of minimizing variations in the offset level and sensitivity of the recorded corneoretinal potentials. The subject was then seated in the PAR device and the head held in fixed constraint on the rotational center by means of a vacuum-operated bladder assembly individually fitted to the head contours of the subject. Calibration of the nystagmus measurement was achieved by the sequential fixation of the eyes on a visual target assembly requiring  $\pm 20$  deg eye displacement. Nystagmus recording was not started until after the first 60 seconds of rotation so as to approach steady-state response conditions. Performance of mental arithmetic problems was required of the subject during the actual recording period in an attempt to enhance his state of alertness. Upon completion of a given run, the nystagmus calibration procedure was repeated with the average of the pre- and post-calibrations used to establish a measurement reference for nystagmus amplitude.

## RESULTS AND DISCUSSION

In the interpretation of the results of this study, it is essential to recognize the basic structure of the experiment. First, relative to the stimulus element of the study, device rotation occurred about an Earth-vertical axis with the subject positioned and oriented so that his z head axis was at the rotational center of the device and in alignment with the rotation axis. Device rotation was programmed to produce continuous sinusoidal motion at nine different, octave-separated frequencies with peak velocity held constant at 50 deg/sec. Accordingly, as stimulus frequency increased, peak

angular acceleration increased and peak angular displacement decreased. In the torsion pendulum context of semicircular canal function, the theoretical effect of this constant-velocity stimulus condition would be to equalize the peak displacements of the cupula-endolymph system occurring at the higher stimulus frequencies. Relative to the response element of the study, nystagmus data were not collected until at least 60 seconds had elapsed from the time of rotation onset in an effort to approach steady-state response conditions. A further point is that during the recording interval, the subject was in the dark with eyes open and thus not provided with any form of visual fixation reference. In this respect, the oculovestibular system was operated open-loop without direct visual feedback and driven under passive conditions in that the environment, rather than the subject, originated the oscillatory motions of the head. Lastly, when evaluating the normative nature of the response data to be presented, consideration must be made of the fact that special response criteria were used for selection of the individuals comprising the study group.

The general characteristics of the horizontal (yaw) nystagmus response to sinusoidal rotation about the z head axis are illustrated by the data presented in Figures 1 and 2. DC corneoretinal potential recordings of the nystagmus response of a single subject are shown for eight octave-separated frequencies ranging from 0.01 to 1.28 Hz. In each figure, the waveform of the PAR tachometer signal is shown immediately above the related nystagmus record. Direction, time, and amplitude relationships are shown at the bottom in each figure. In conformance with the results of earlier work (refs. 11 and 8) each reversal in the direction of the rotational stimulus is accompanied by a reversal in the direction of the nystagmus response; the waveform of the slow-component (slow-phase) eye velocity signal is sinusoidal over the entire stimulus region; at the higher stimuli frequencies, the waveform of the slow-component eye displacement signal proper becomes sinusoidal with minimal distortion due to fast-component incidence; the waveform of the fast-component (fast-phase) eye velocity signal describes a heavily clipped sinusoid in that its peak velocity appears to saturate early in each cycle but to diminish in magnitude to either side of the nystagmus transitions; and that the nystagmus transitions lag the directional transitions of the angular acceleration stimulus with the lag being smallest at the lower stimulus

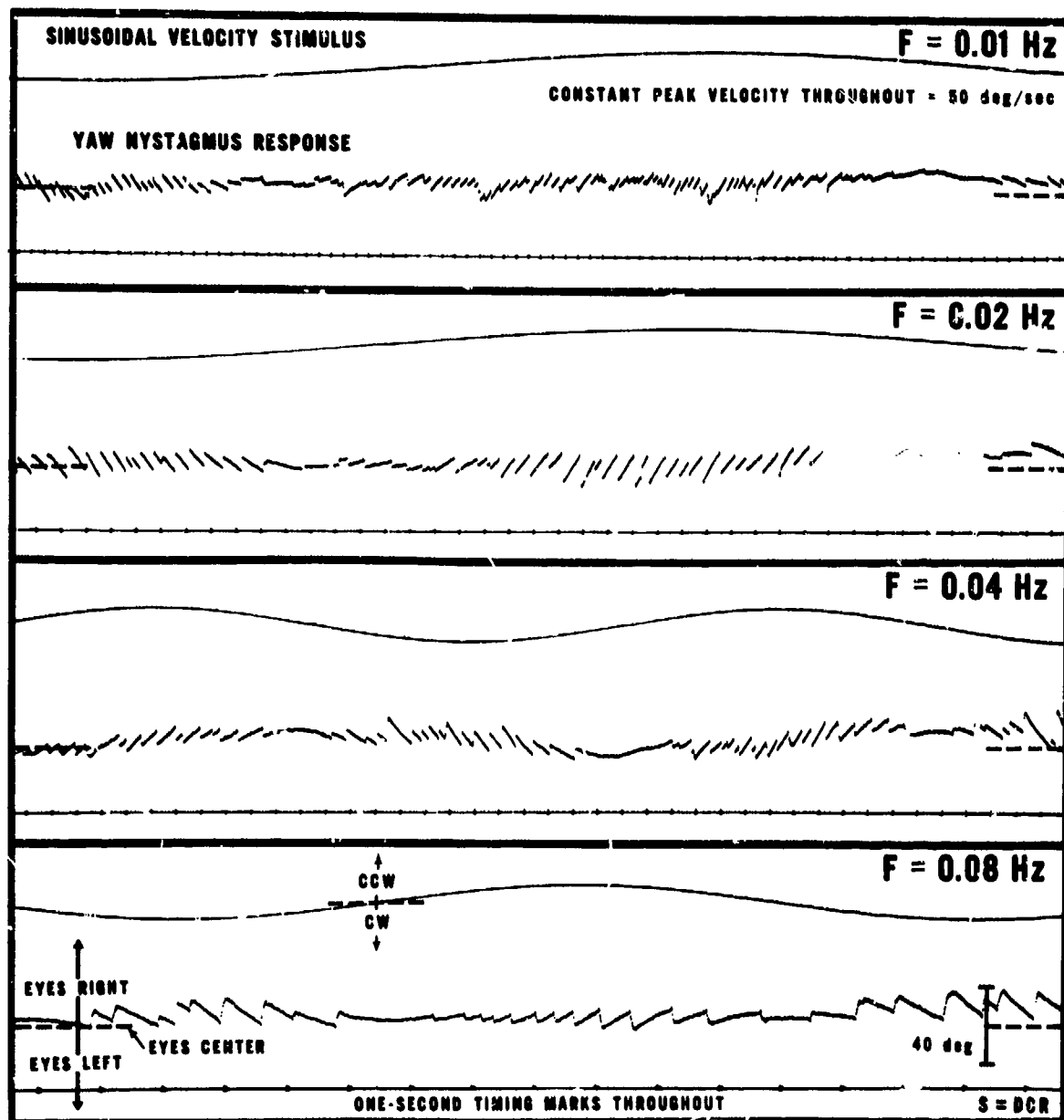


Figure 1

DC corneoretinal potential recording of horizontal eye position showing the nystagmus response of a single subject as elicited by yaw angular oscillation of the head at four different octaves-separated frequencies covering the 0.01 to 0.08 Hz spectrum. The peak angular velocity of the head was maintained constant at 50 deg/sec throughout the spectrum.

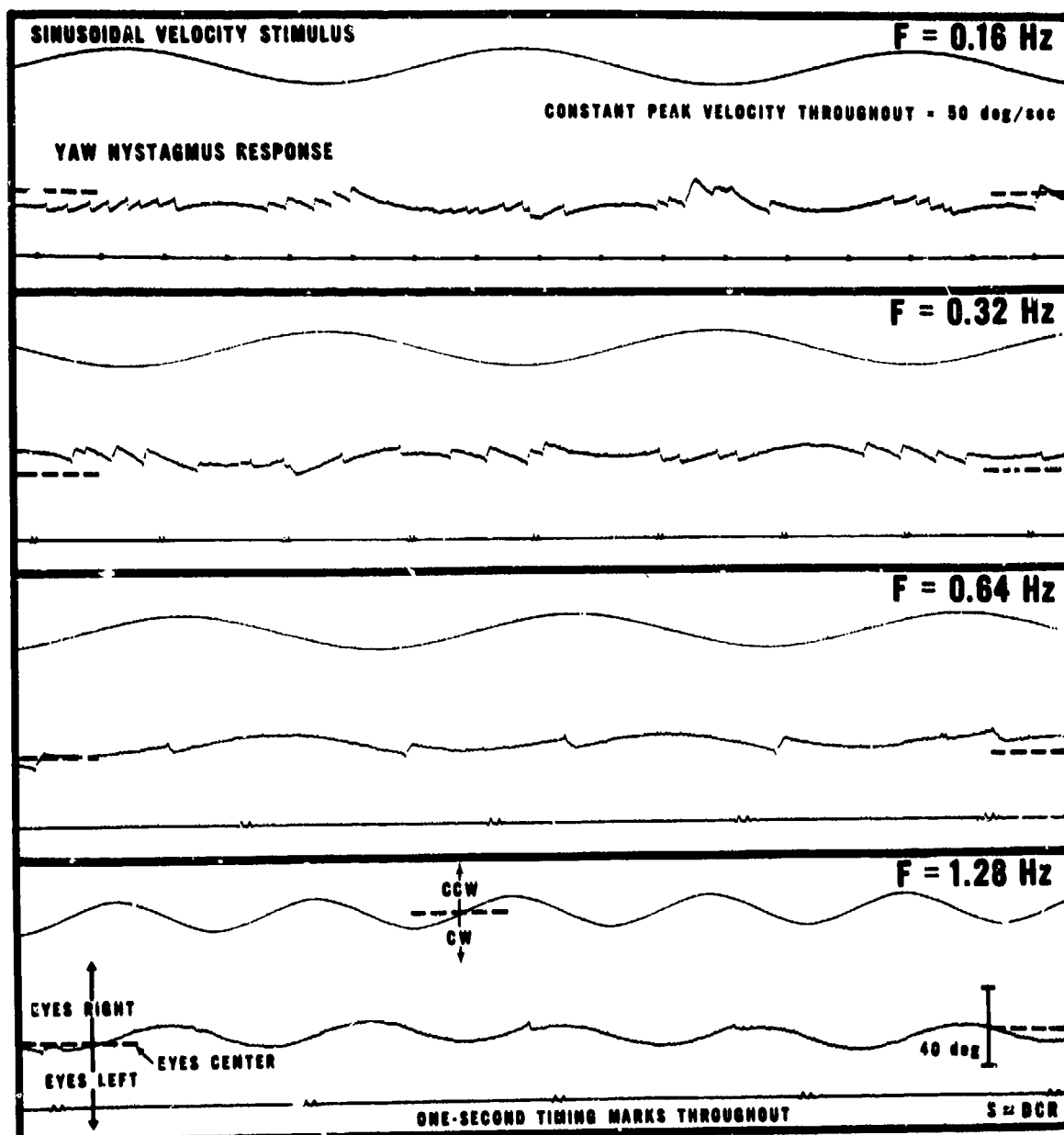


Figure 2

Same as Figure 1 except stimulus frequencies cover the 0.16 to 1.28 Hz spectrum. Note the virtual disappearance of fast components (beats) in the nystagmus response observed at 1.28 Hz.

frequencies and approaching 90 deg (180 deg out of phase with the head angular velocity) at the higher stimulus frequencies. A slight trend for the phase angle to decrease as a function of stimulus duration was observed at the lower stimulus frequencies. (Pilot data indicate that for prolonged continuous oscillation, considerable shift can occur, for example, a 6-deg phase decrement following 30 min of rotation at 0.04 Hz.)

The sinusoidal nature of the eye displacement signal proper at the higher stimulus frequencies is well illustrated by the 1.28 Hz recording presented in Figure 2. At this frequency, sinusoidal nystagmus occurred without the presence of a fast component for a considerable number of cycles for each of the ten subjects. Of twenty half-cycle nystagmus response periods scored for each subject, the mean incidence of response periods without any recognizable fast components was 10.9; i.e., approximately 55 percent of the response cycles were free of fast-component "perturbations" of the sinusoidal displacement waveform. Another observation concerns the mean beat-frequency of the nystagmus as a function of frequency. For each subject, the number of beats occurring within each cycle of the response was counted and the mean number of beats per second calculated, using the cyclic period as the time base. The combined means for the ten subjects are plotted in Figure 3 as a function of the stimulus frequency. Interestingly,

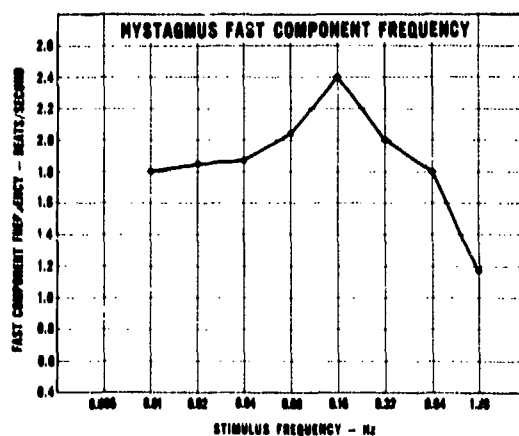


Figure 3

Plot of the mean beat frequency of the nystagmus fast components as a function of the stimulus frequency showing an unexpected peak at 0.16 Hz.

the nystagmus beat frequency rose in the mid-band region and peaked at 0.16 Hz before beginning its expected high-frequency roll-off.

The measurement references and related nomenclature used to calculate the phase and amplitude data which follow are summarized in Figure 4. A tracing of a typical nystagmus response to a sinusoidal stimulus (0.08 Hz in this case) is shown at the bottom in this figure. Immediately above, the stimulus is defined in terms of the instantaneous angular acceleration, angular velocity and angular displacement of the head where the cyclic period of each oscillation (equivalent to 360 electrical deg) is measured as T sec. Under steady-state conditions, the directional transitions in the velocity waveform lag the corresponding transitions in the acceleration waveform by 90 deg, and the displacement waveform is 180 deg out of phase with the acceleration

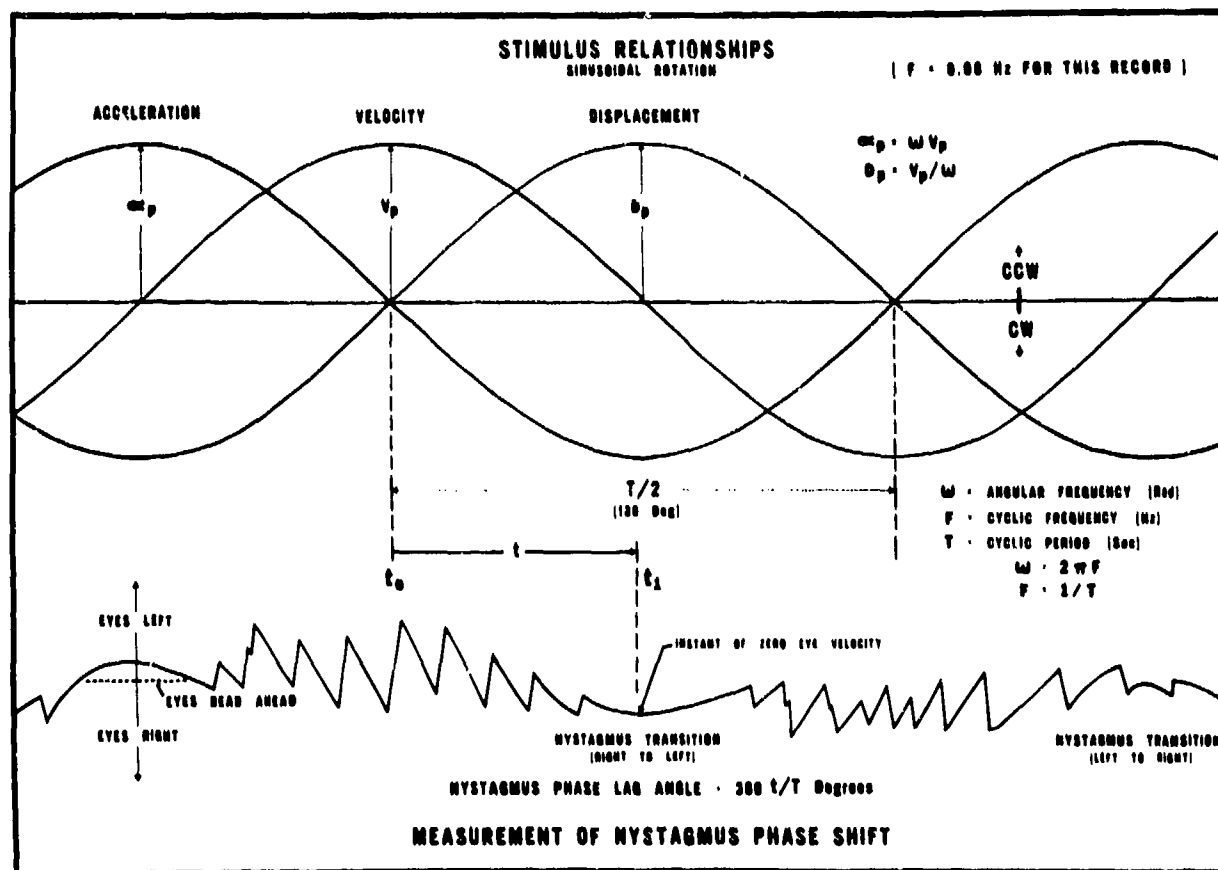


Figure 4

Measurement procedures used to identify and score the phase angle defined by the time difference between reversals in the direction of the angular acceleration stimulus and the following reversals in the direction of the elicited nystagmus response.



waveform. Since the nystagmus record is a measure of the instantaneous displacement rather than velocity of the eyes, the reversal in direction of the nystagmus response is at the point of zero slope of the displacement record. The actual magnitude of the nystagmus phase lag is measured as follows: Referring to Figure 4, consider the oscillation interval immediately preceding the time denoted as  $t_0$ . During this interval, the subject is being angularly accelerated in the counterclockwise direction, thus resulting in nystagmus with a slow-component velocity to the right. At time  $t_0$  the acceleration stimulus reverses direction. The slow-component eye velocity then begins to decrease, reaches zero velocity at time  $t_1$ , and then begins to increase in level but in the opposite direction. The phase difference between this nystagmus transition and the stimulus transition is quantified by measuring the lag time  $t$ , the cyclic period  $T$ , and calculating the nystagmus phase angle as  $360 t/T$  deg. The phase angle for the transition depicted in this figure is approximately 90 deg. For the amplitude analysis, peak eye velocity was measured for each half-cycle at the midpoint of the two related transitions. It follows that two phase and two amplitude measures were obtained for each stimulus cycle.

Using these procedures, the mean nystagmus phase angle and the mean peak eye velocity were separately calculated for each subject at each of the nine frequencies. These individual means were then combined to calculate the group means, standard deviations and standard errors of the mean as summarized in Table II. These phase and amplitude data are separately plotted in Figure 5 as a logarithmic function of frequency. In the case of the amplitude data, the mean peak eye velocity is plotted on both a logarithmic and linear basis.

As a matter of convenience to the discussion of the frequency characteristics of these data, reference will be made to Table II which lists various equivalent linear second-order equations commonly used to describe the transduction action of the semicircular canals in terms of the heavily-damped torsion pendulum analog. These equations treat the instantaneous inertial angular acceleration of the skull as the driving stimulus and the resulting instantaneous angular displacement of the cupula-endolymph system measured relative to the skull as the elicited response. The notation of equation A (refs. 6 and 14) expresses the transduction process in terms of the theoretical physical

TABLE II  
Horizontal Ocular Nystagmus Phase Lag and Peak Eye Velocity as a Function of Frequency  
- Based on Individual Means of 10 Subjects -

Stimulus Frequency-Hz	0.005	0.01	0.02	0.04	0.08	0.16	0.32	0.64	1.28
Group Mean Phase Lag (deg)	13	41	63	76	84	85	88	89	89
Standard Deviation of Means	9.6	6.4	5.0	5.4	4.6	3.2	2.5	2.8	2.8
Standard Error of Mean	3.0	2.0	1.6	1.7	1.5	1.0	0.8	0.9	0.9
Group Mean Peak Eye Velocity (deg/sec)	11	21	24	24	29	31	33	36	45
Standard Deviation of Means	4.0	6.3	5.0	7.0	6.7	8.7	10.4	11.0	7.8
Standard Error of Mean	1.3	2.0	1.6	2.2	2.1	2.8	3.3	3.5	2.5

characteristics of the cupula-endolymph system; equation B derives from conventional control theory representation of a second-order system and describes performance in terms of generalized damping ratio and natural frequency coefficients; and equations C and D are related transfer function oriented expressions that define the response in terms of either system time-constants or related break/corner frequencies. The equivalency of these equations is established by the coefficient relationships listed in equation sets E, F, and G. In general, the magnitude of a vestibular response to motion is considered to be a function of the magnitude of the cupula-endolymph displacement produced by the stimulus. For the nystagmus response it is convention to link, in one form or another, the angular velocity of the eyes during the slow component to the angular displacement of the cupula-endolymph system.

From the frequency viewpoint, equation set D is of advantage to this study since the steady-state cupula-endolymph response to periodic sinusoidal angular acceleration stimuli of variable frequency is described in terms of two break or corner frequencies,  $\omega_1$  and  $\omega_2$ . If an experimental determination can be made of these two frequencies, numerical values will be established for the long and short time constants,  $T_1$  and  $T_2$ ,

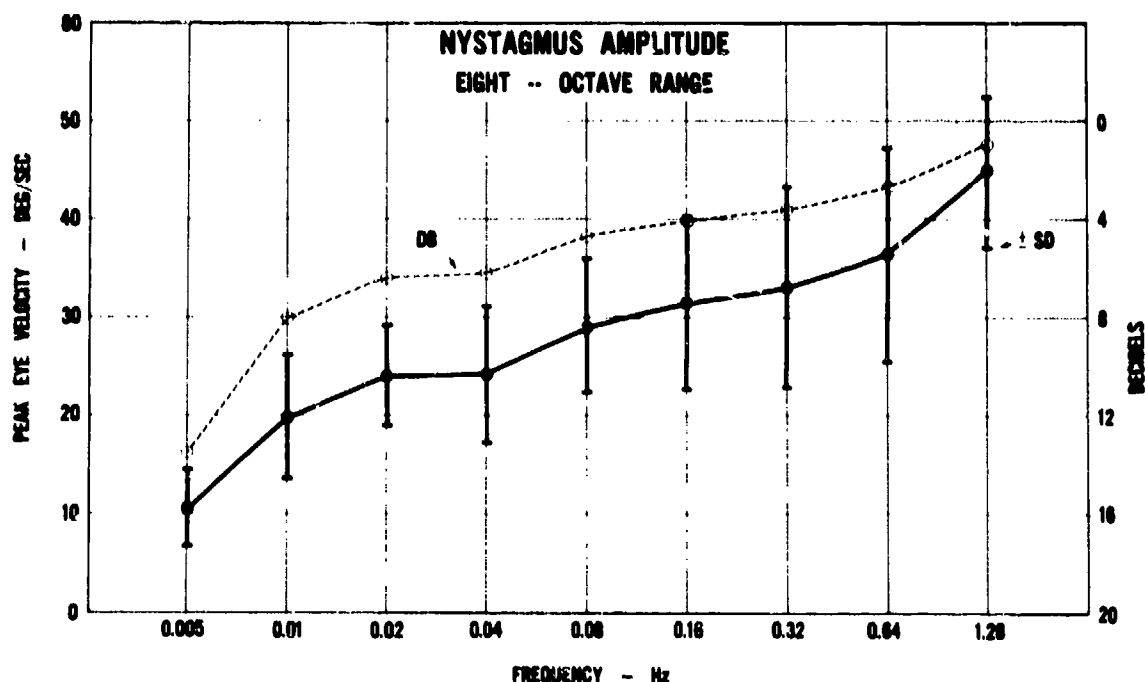
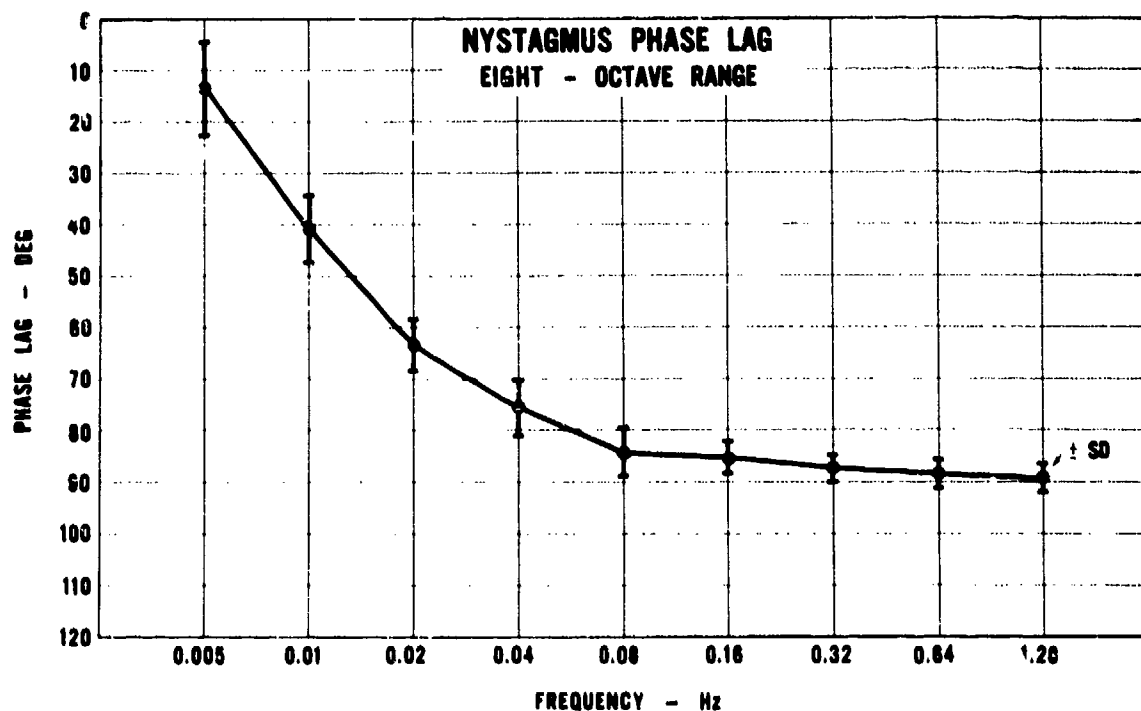


Figure 5

Plot of the mean nystagmus phase shift (upper) and mean peak slow-component eye velocity (lower) as a logarithmic function of frequency for the 10-subject study group. The amplitude of the velocity response is plotted on a logarithmic as well as linear basis. Note that the variability of the amplitude data is considerably greater than that of the phase data as denoted by the +/- one standard deviation bar plotted at each datum.

as well as the  $\Theta$ ,  $\Pi$ , and  $\Delta$  coefficients. The response of the cupula-endolymph system to variable frequency stimuli with peak acceleration held constant can be summarized in terms of these corner frequencies as follows: At stimulus frequencies much lower than  $\omega_1$ , the sinusoidal deflections of the cupula-endolymph will be in phase with the acceleration waveform and have a peak amplitude proportional to the peak acceleration level of the stimulus. The response will depart from this constant-gain mode as  $\omega_1$  is approached in that the cupula-endolymph displacements will begin to fall in amplitude and lag behind the acceleration stimulus. When the stimulus frequency equals  $\omega_1$ , the phase lag will be 45 deg and the amplitude down 3 db from its value in the constant-gain region. As the frequency is raised beyond  $\omega_1$ , the phase lag will continue to increase and the amplitude response will fall off at a 6 deg/octave rate. When the upper corner frequency  $\omega_2$  is reached, the phase lag will have increased to 135 deg. Beyond  $\omega_2$ , the amplitude will fall off at a 12 deg/octave rate and the phase lag asymptotically approach 180 deg. A third frequency of experimental interest is the undamped characteristic angular frequency  $\omega_n$  which marks the logarithmic midpoint between  $\omega_1$  and  $\omega_2$ . This frequency is determined as the point where the phase response passes through 90 deg. For a heavily damped system, the Table III equations also require the phase response to be relatively constant in the immediate vicinity of  $\omega_n$ . In essence, if an experimental determination can be made of any two of these three frequencies, it becomes possible to calculate numerical values for each of the coefficients listed in Table III.

When the peak velocity rather than peak acceleration of the stimulus is maintained constant as was done in this study, the phase relationships remain as described above. The amplitude response is as follows: In the mid-band region between  $\omega_1$  and  $\omega_2$ , the peak angular displacements of the cupula-endolymph system will be proportional to the peak angular velocity of the stimulus and thus independent of the stimulus frequency. In this constant-gain region, the phase shift approximates 90 deg, and the sinusoidal displacements of the cupula-endolymph will be in phase on a compensatory basis with the sinusoidal waveform describing the instantaneous angular velocity of the skull. If the angular velocity of the eyes during the slow component of nystagmus is made proportional to cupula-endolymph displacement, the eye velocity waveform is predicted to be in phase on a compensatory basis with the skull velocity waveform in

**TABLE III**  
**THEORETICAL CUPULA-ENDOLYMPH RESPONSE TO ANGULAR ACCELERATION**  
 Listing of equivalent linear second-order differential equation representations

**CONVENTIONAL PHYSICAL CHARACTERISTICS REPRESENTATION**

$$\ddot{\xi} + \frac{\pi}{\Theta} \dot{\xi} + \frac{\Delta}{\Theta} \xi = \alpha(t) \quad \xi \equiv \xi(t) \quad \text{A}$$

$\xi, \dot{\xi}, \ddot{\xi}$  = Instantaneous angular displacement, velocity, and acceleration of the cupula-endolymph system relative to the skull.  
 $\Theta, \pi, \Delta$  = Equivalent rotational mass, resistance (viscous damping) and stiffness of the cupula-endolymph system.  
 $\alpha(t)$  = Instantaneous angular acceleration of the skull.

**CONVENTIONAL CONTROL THEORY REPRESENTATION**

$$\ddot{\xi} + 2\zeta\omega_n \dot{\xi} + \omega_n^2 \xi = \alpha(t) \quad \text{B}$$

$\zeta$  = Equivalent damping ratio of cupula-endolymph system.  
 $\omega_n$  = Equivalent undamped characteristic angular frequency (natural frequency) where  $\omega_n = 2\pi F_n$  rad/sec,  $F_n = \text{Hz}$ .

**CONVENTIONAL TIME-CONSTANT REPRESENTATION**

$$\ddot{\xi} + \frac{1}{T_2} \dot{\xi} + \frac{1}{T_1 T_2} \xi = \alpha(t) \quad \text{C}$$

$T_1$  = Long time-constant of cupula-endolymph system.  
 $T_2$  = Short time-constant of cupula-endolymph system.

**CONVENTIONAL SYSTEM TRANSFER FUNCTION REPRESENTATIONS**

$$\frac{\xi(s)}{\alpha(s)} = \frac{1}{(s + 1/T_1)(s + 1/T_2)} = \frac{1}{(s + \omega_1)(s + \omega_2)} \quad \omega = 2\pi F \quad \text{D}$$

$\omega_1, F_1$  = Lower corner-frequency of cupula-endolymph system.  
 $\omega_2, F_2$  = Upper corner-frequency of cupula-endolymph system.

**COEFFICIENT RELATIONSHIPS FOR ABOVE EQUATIONS**

$$\frac{\pi}{\Delta} = \frac{2\zeta}{\omega_n} = T_1 = \frac{1}{\omega_1} = \frac{1}{2\pi F_1} \quad (\text{sec}) \quad \text{E}$$

$$\frac{\Theta}{\Delta} = \frac{1}{2\zeta\omega_n} = T_2 = \frac{1}{\omega_2} = \frac{1}{2\pi F_2} \quad (\text{sec}) \quad \text{F}$$

$$\frac{\Theta}{\Delta} = \frac{1}{\omega_n^2} = T_1 T_2 = \frac{1}{\omega_1 \omega_2} = \frac{1}{(2\pi F_n)^2} \quad (\text{sec}^2) \quad \text{G}$$

this  $\omega_1$  to  $\omega_2$  region. Unity gain arrives when the peak velocity of the eyes during the slow component equals the peak velocity of the stimulus. At stimulus frequencies above and below the constant-gain region, the equations predict a 6 db/octave roll-off of the amplitude response.

Returning to the nystagmus data presented in Figure 5, it can be seen that at the lower stimulus frequencies the phase data follow, in general, the predictions of the Table III equations as just discussed. At 0.005 Hz a nystagmus phase lag of only 13 deg was observed, indicating that the waveform of the slow-component eye velocity was very nearly in phase with the waveform of the acceleration stimulus. As frequency was raised, the phase angle also increased approaching 90 deg at the higher stimulus frequencies, thus signifying a nearly one-to-one compensatory phase relationship with skull velocity. Since the range of nystagmus phase angles observed at the lower frequencies allows interpolation of the 45-deg phase crossover frequency, it appears that the stimulus range was adequate to allow an experimental determination of the lower corner frequency  $\omega_1$ . It is quite obvious, however, that the high frequency stimulus region was not at all adequate to either define a value for the upper corner frequency,  $\omega_2$ , or to even establish its very existence. Similarly, since the phase curve did not cross the 90-deg contour, neither can the phase data be used to arrive at an experimental determination of the natural frequency  $\omega_n$ . This finding contradicts earlier work (ref. 11) where, using a different rotator that was limited to a maximum stimulus frequency of 0.2 Hz, it was predicted that the 90-deg phase crossover would occur before reaching the 1.28 Hz limit of the present study.

Referring now to the amplitude data of Figure 5, the response decrement observed at the low end of the stimulus spectrum is in general agreement with the response predictions associated with the lower corner frequency  $\omega_1$ . The amplitude response observed at the higher stimulus frequencies, however, offer considerable conflict with the predictions of the Table III equations. Except for the single octave between 0.02 and 0.04 Hz, the amplitude response can be seen to rise as frequency is raised instead of remaining constant. Though the peak velocity of the stimulus was maintained constant at 50 deg/sec, unity gain was not reached even at the maximum stimulus frequency of 1.28 Hz. In effect, the compensatory velocity motions of the eye were not adequate to

stabilize the inertial position of the eyes in this stimulus region even though the eye velocity and head velocity waveforms were in relatively good phase agreement.

This observed rise in the amplitude response as frequency is raised supports the findings of Benson (ref. 2) who extended the upper stimulus range to 5.0 Hz. His data indicate that amplitude continues to rise throughout the 0.5 to 5.0 Hz region. Significantly, he found that the response involved gain-enhancement in that the peak eye velocity actually exceeded the peak velocity of the skull at the upper end of his stimulus range. Equally important, his phase data at the higher stimulus frequencies remained constant at approximately 90 deg even though gain continued to rise out to the 5.0 Hz limit. In contradistinction to the results of this study, Benson did observe, however, a stimulus region (0.05 to 0.5 Hz) where the amplitude response of his subjects remained constant. Though an account for this difference cannot be provided at the present time, the Benson observation is in better agreement with the present concept of cupula-endo-lymph behavior.

This rise in gain at the higher frequencies, signifying the presence of a lead term in the over-all transfer function, has also been observed by Fernandez and Goldberg in a comprehensive series of experiments (refs. 3, 4, and 5) dealing with afferent impulses recorded in the vestibular nerve of the squirrel monkey. Using sinusoidal stimuli, they detected and quantitatively described the presence of a high-frequency lead term which was postulated to derive from a cupula velocity source. Importantly, the rise in gain they observed at the higher stimulus frequencies was accompanied by a corresponding decrease in phase lag which would be expected when the corner frequency of the lead term is less than the upper frequency  $\omega_2$ . With the phase data of this study and the phase data of the Benson study, the phase change predicted by such a lead term was not observed. Formal introduction of the lead term into the nystagmus transfer function will require resolution of this apparent gain-phase conflict. Further work in this direction is being conducted by Barnes and Benson (ref. 1) who have introduced a lead term combined with a neural integrator to model the saccade features of the nystagmus response.

Returning to the low-frequency phase data of Figure 5, a preliminary estimate of the lower corner frequency  $\omega_1$  derives from the 45-deg crossover frequency. Defining

the experimentally measured nystagmus phase lag angle as  $\phi$ , the denoted crossover establishes the following:

$$\begin{aligned} \text{For } \phi &\approx 45 \text{ deg, } F \approx 0.012 \text{ Hz} && (\text{From Figure 5 raw data}) \\ \omega_1 &\approx 0.077 \text{ rad/sec} \\ \frac{\pi}{\Delta} &\approx T_1 \approx 13.3 \text{ sec} \end{aligned}$$

A conflict arises, however, if this value of  $\omega_1$  is used to calculate the theoretical phase shift expected at adjoining frequencies. When the calculated phase angles are compared to the observed values of  $\phi$ , it is found that the theoretical values overestimate the observed phase shift with the deviation being greatest at the lower frequencies. In effect, the slope of the observed data is found to be greater than that predicted by a simple first-order, low-pass filter of corner frequency  $\omega_1$ .

This deviation of the observed phase data also becomes apparent when one uses an alternative approach to the determination of  $\omega_1$ . As has been described previously (ref. 11) the phase response of a heavily-damped system that is operated at a frequency much lower than its natural frequency can be approximated as

$$\phi \approx \arctan \left( \frac{\omega}{\omega_1} \right) \approx \arctan (\omega T_1)$$

In the experimental situation where  $\phi$  can be measured in response to a known stimulus frequency  $\omega = 2 \pi F$ , it follows that  $\omega_1$  and its related coefficients can be calculated as:

$$T_1 = \frac{1}{\omega_1} \approx \frac{\pi}{\Delta} = \frac{\tan \phi}{2 \pi F}$$

Using this approach, a value for  $T_1$  was calculated at each of the four lowest stimulus frequencies. The results, shown plotted in Figure 6, indicate that the long-time constant  $T_1$ , or equivalently  $\pi/\Delta$ , varies as a function of frequency, a direct conflict with the predicted behavior of a linear system. This potential nonlinearity would not be expected to arrive as a result of stimulus intensity (ref. 8) since the constant-velocity stimulus condition of the study produced very low acceleration levels (Table 1) at the lower end of the spectrum. A much more probable cause is the low-frequency phase lead introduced by adaptation effects. In effect, the link between the theoretical output of the cupula-endolymph system and the resulting nystagmic eye motions must take into account the gradual decrement in response that always occurs during exposure to long-duration acceleration stimuli.



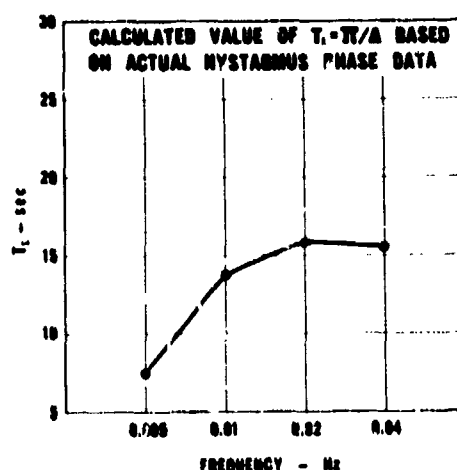


Figure 6

Plot of calculated values for the long time constant,  $T_L$ , of the cupula-endlolymph system based on the raw phase data of Figure 5 and the assumption that the denoted stimulus frequencies are much lower than the natural frequency of the system. Note the apparent nonlinearity as a function of stimulus frequency.

A system transfer function representation of this effect has been well defined by Young and Oman (ref. 15) and Malcolm and Jones (ref. 10) who independently synthesized near-identical adaptation models that account for both the response decrement noted above and the secondary vestibular responses that arise following termination of long-duration, unidirectional acceleration stimuli. In the notation of Young and Oman, the vestibular output signal  $R(t)$  produced by a given cupula displacement signal  $\xi(t)$  is modified by adaptation according to the system transfer function

$$\frac{R(s)}{\xi(s)} = \frac{s}{(s + 1/T_a)} \quad (\text{Young and Oman - ref. 15})$$

where  $T_a$  is the adaptation time constant. From the frequency viewpoint, this adaptation model describes a high-pass filter with a corner frequency of  $\omega_a = 1/T_a$ . The effect of the model is to introduce a first-order phase lead in the vestibular response at very low stimulus frequencies with the extent of the lead present at a given frequency dependent on the value of  $T_a$ .

The theoretical phase lead produced by the model at the four lower stimulus frequencies of this study for three different values of the time constant,  $T_a$ , is shown in Figure 7. Since the raw phase data of Figure 5 would supposedly define the net effect

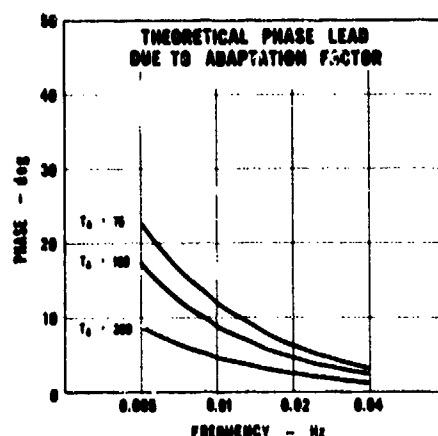


Figure 7

Theoretical phase lead introduced by the adaptation model (Malcolm and Jones - ref. 10, Young and Chan - ref. 15) at the four lower stimulus frequencies of this study for three different values of the adaptation time constant,  $T_A$ .

of the cupula-endolymph phase lag and the adaptation phase lead acting in combination, a measure of the phase lag due to only the cupula-endolymph mechanics could be postulated by adding the adaptation phase lead angles for a given time constant  $T_A$  to the raw data of Figure 5. This procedure was followed at each of the four lower stimulus frequencies and the resulting "corrected" phase angles used to again calculate  $T_1$  according to the method of Figure 6. The results of these calculations, plotted in Figure 8, indicate that the  $T_1$  nonlinearity observed in Figure 6 is fairly well "corrected" by the 100-sec adaptation time constant.

The phase-frequency curve, which results when the phase-lead effects of the 100-sec adaptation model are removed from the raw nystagmus phase shift data, is shown plotted in dashed outline in Figure 9. The frequency at which this dashed curve crosses the 45-deg phase contour allows the lower corner frequency,  $F_1$ , to be estimated as 0.0085 Hz. This is considerably lower than the 0.02 Hz estimate gained from the raw phase data. As shown below, the associated estimate

$$\text{For } \phi = 45 \text{ deg, } F_1 = 0.0085 \text{ Hz} \quad (\text{From Figure 9, } T_A = 100 \text{ sec})$$

$$\omega_1 = 0.053 \text{ rad/sec}$$

$$\frac{\pi}{\Delta} = T_1 = 19 \text{ sec}$$

of  $T_1$  is in good agreement with the values calculated in Figure 8 using the same 100-sec adaptation time constant.

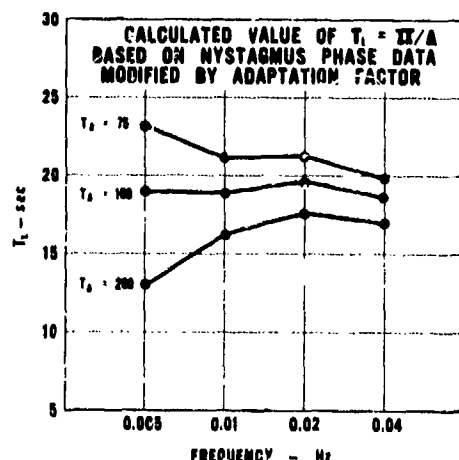


Figure 8

Same as Figure 6 except calculations of  $T_1$  based on modification of the raw phase data according to the phase lead introduced by the three adaptation time constants specified in Figure 7. A time constant of 100 sec achieves a reasonable correction of the nonlinearity observed in Figure 6.

To summarize, a reasonable description of the low-frequency phase data results when an adaptation time constant of  $T_a \approx 100$  sec is combined with a cupula-endolymph long time constant of  $T_1 \approx 19$  sec in the over-all transfer function for the nystagmus response. The denoted value for the adaptation time constant is also compatible with values found by other investigators (refs. 10, 13, and 15) using the same model but different stimuli. When the long time constant was estimated from the raw phase data without considering the adaptive term, a significantly lower value of 13 sec resulted. This underestimate fully supports the contention of Malcolm and Jones (ref. 10) that determinations of  $T_1$  based on data that do not take adaptation into account will be considerably lower than those gained through inclusion of the term.

The  $T_a \approx 100$  sec and  $T_1 \approx 19$  sec time constants are related to corner frequencies of  $F_a \approx 0.0016$  Hz and  $F_1 \approx 0.0085$  Hz, respectively. When the driving torque to the semicircular canals is maintained constant, i.e., when the peak angular acceleration of the skull is held constant, the response is predicted to fall off at stimulus frequencies to either side of these two corner frequencies. In effect, the frequency

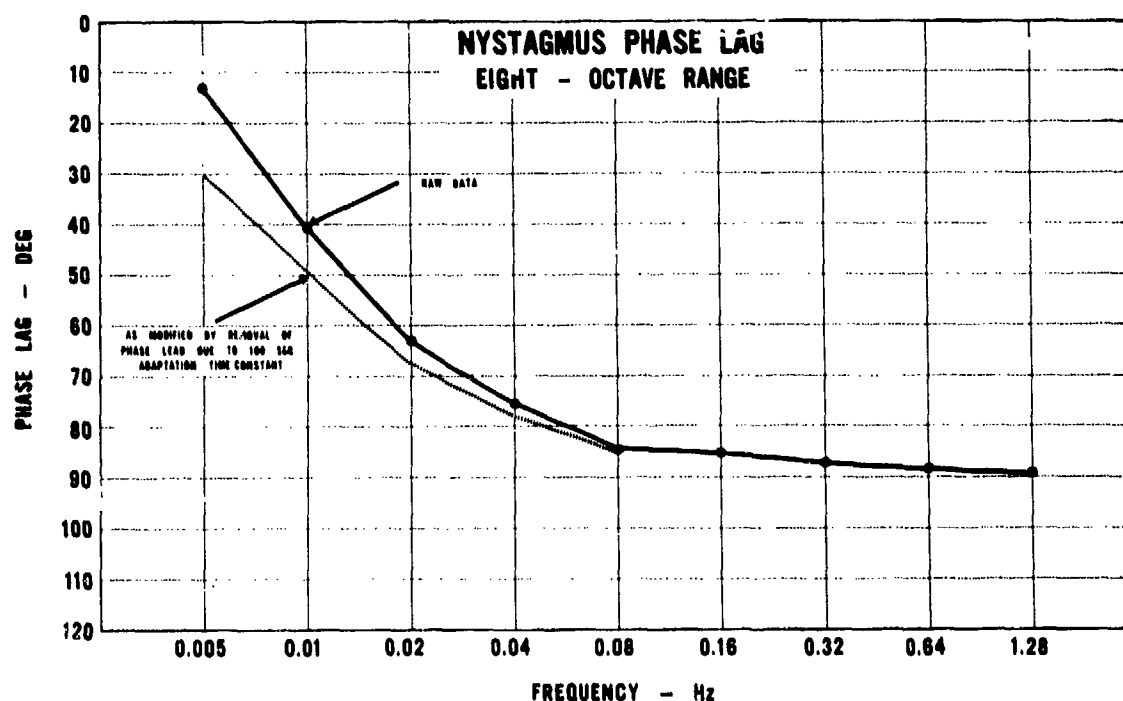


Figure 9

Plot of the raw phase data of Figure 5 (solid outline) as modified by removal of the phase-lead effects of the adaptation model based on an adaptation time constant of 100 sec (dashed outline). The modified phase data allow the lower corner frequency of the cupula-endolymph system to be estimated as 0.0085 Hz. The resulting  $T_1 \approx 19$  sec estimate for the long time constant of the system is in agreement with the Figure 8 estimates using the same 100-sec adaptation time constant.

band between 0.0016 and 0.0085 Hz would be considered to define the most sensitive nystagmus response region. Though the Figure 5 amplitude data seem to signify that the response was greatest at the higher stimulus frequencies, the peak acceleration level at 1.28 Hz was actually 256 times greater than the peak level at 0.005 Hz since the peak velocity of the stimulus was maintained constant across the spectrum.

A last point involves the operational interpretation of the nystagmic eye motions elicited by such ycw stimuli. As discussed earlier, the stimulus range where the nystagmus phase lag approaches 90 deg defines a situation where the angular velocity of the eyes during the slow component of nystagmus is in phase, on a compensatory basis, with the angular velocity of the head. The effect is to more or less stabilize eye position so that gaze can be maintained on an external reference fixed in space, that is, on a

point not fixed or attached to the device or vehicle producing the yaw motions. For a visual reference fixed to the vehicle, such as a cockpit instrument or display, the elicited nystagmus would always produce relative movement between the eyes and the visual reference. Although the extent of the relative movement can be reduced somewhat by wilful fixation on the instrument or display, degradation of visual performance will still be a primary result of such stimulation.

## REFERENCES

1. Barnes, G. R., and Benson, A. J., A model for the prediction of the nystagmic response to angular and linear acceleration stimuli. In: The Use of Nystagmography in Aviation Medicine. AGARD-CP-128. London: Technical Editing and Reproduction Ltd., 1973. Pp A23-1 - A23-13.
2. Benson, A. J., Interactions between semicircular canals and gravireceptors. In: Busby, D. E. (Ed.), Recent Advances in Aerospace Medicine. Dordrecht: D. Reidel Pub. Co., 1970. Pp 249-261.
3. Fernandez, C., and Goldberg, J. M., Physiology of peripheral neurons innervating semicircular canals of the squirrel monkey: II. Response to sinusoidal stimulation and dynamics of peripheral vestibular system. J. Neurophys., 34:661-675, 1971.
4. Goldberg, J. M., and Fernandez, C., Physiology of peripheral neurons innervating semicircular canals of the squirrel monkey: I. Resting discharge and response to constant angular accelerations. J. Neurophys., 34:635-660, 1971.
5. Goldberg, J. M., and Fernandez, C., Physiology of peripheral neurons innervating semicircular canals of the squirrel monkey: III. Variations among units in their discharge properties. J. Neurophys., 34:676-684, 1971.
6. Groen, J. J., The semicircular canal system of the organs of equilibrium: I and II. Physics in Med. Biol., 1:103-117 and 225-242, 1956-57.
7. Hixson, W. C., and Niven, J. I., Application of the system transfer function concept to a mathematical description of the labyrinth. I. Steady-state nystagmus response to semicircular canal stimulation by angular acceleration. NSAM-458. Pensacola, FL: Naval School of Aviation Medicine, 1961.
8. Hixson, W. C., and Niven, J. I., Frequency response of the human semicircular canals. II. Nystagmus phase shift as a measure of nonlinearities. NSAM-830. Pensacola, FL: Naval School of Aviation Medicine, 1962.
9. Hixson, W. C., and Niven, J. I., A torque motor servomotor for vestibular application. NAMI-979. Pensacola, FL: Naval Aerospace Medical Institute, 1966.
10. Malcolm, R., and Melvill-Jones, G., A quantitative study of vestibular adaptation in humans. Acta otolaryng. (Stockh.), 70:126-135, 1970.
11. Niven, J. I., and Hixson, W. C., Frequency response of the human semicircular canals: I. Steady-state ocular nystagmus response to high-level, sinusoidal angular rotations. NSAM-459. Pensacola, FL: Naval School of Aviation Medicine, 1961.

12. Niven, J. I., Hixson, W. C., and Correia, M. J., An experimental approach to the dynamics of the vestibular mechanisms. In: The Role of the Vestibular Organs in the Exploration of Space. NASA SP-77. Washington, D. C.: U. S. Government Printing Office, 1965. Pp 43-56.
13. Stockwell, C. W., Gilson, R. D., and Guedry, F. E., Adaptation of horizontal semicircular canal responses. Acta otolaryng. (Stockh.), 75:471-476, 1973.
14. van Egmond, A.A.J., Groen, J. J., and Jongkees, L.B.W., The mechanics of the semicircular canal. J. Physiol. (Lond.), 110:1-17, 1949.
15. Young, L. R., and Oman, C. M., Model for vestibular adaptation to horizontal rotation. Aerospace Med., 40:1076-1080, 1969.

Hixson, W. Carroll

1974

FREQUENCY RESPONSE OF THE OCULOVESTITIBULAR SYSTEM DURING YAW OSCILLATION. NAMRL-1212. Pensacola, FL: Naval Aerospace Medical Research Laboratory, 8 December.

The report describes the results of a system transfer function study of the oculovestitibular response to yaw oscillation. Ten naval aviator candidates were exposed to Earth-vertical rotation about the z head axis at nine different octave-separated frequencies covering the 0.005 to 1.28 Hz spectrum with peak velocity held constant at 50 deg/sec. The frequency dependence of the oculovestitibular system was interpreted in terms of phase and amplitude measures of the resulting horizontal nystagmus. Though the phase data were observed to deviate somewhat from those predicted by the conventional second-order cupula-endolymph model at the lower stimulus frequencies, a theoretical account for the deviation was provided by introducing an adaptation model as developed by other researchers. An adaptation time constant of 100 sec was found to best represent the observed phase response. By taking into account the phase lead introduced by this factor, the lower corner frequency of the cupula-endolymph system was estimated to be 0.0085 Hz (a long time constant of approximately 19 sec).

Aerospace medicine  
Human effectiveness  
Flight forces  
Angular acceleration  
Labyrinth  
Oculovestitibular system  
Semicircular canals  
Cupula-endolymph system  
Eye motions  
Nystagmus  
Biological models  
Frequency response  
Transfer functions  
Bioengineering

Hixson, W. Carroll

1974

FREQUENCY RESPONSE OF THE OCULOVESTITIBULAR SYSTEM DURING YAW OSCILLATION. NAMRL-1212. Pensacola, FL: Naval Aerospace Medical Research Laboratory, 8 December.

The report describes the results of a system transfer function study of the oculovestitibular response to yaw oscillation. Ten naval aviator candidates were exposed to Earth-vertical rotation about the z head axis at nine different octave-separated frequencies covering the 0.005 to 1.28 Hz spectrum with peak velocity held constant at 50 deg/sec. The frequency dependence of the oculovestitibular system was interpreted in terms of phase and amplitude measures of the resulting horizontal nystagmus. Though the phase data were observed to deviate somewhat from those predicted by the conventional second-order cupula-endolymph model at the lower stimulus frequencies, a theoretical account for the deviation was provided by introducing an adaptation model as developed by other researchers. An adaptation time constant of 100 sec was found to best represent the observed phase response. By taking into account the phase lead introduced by this factor, the lower corner frequency of the cupula-endolymph system was estimated to be 0.0085 Hz (a long time constant of approximately 19 sec).

Aerospace medicine  
Human effectiveness  
Flight forces  
Angular acceleration  
Labyrinth  
Oculovestitibular system  
Semicircular canals  
Cupula-endolymph system  
Eye motions  
Nystagmus  
Biological models  
Frequency response  
Transfer functions  
Bioengineering

Hixson, W. Carroll

1974

FREQUENCY RESPONSE OF THE OCULOVESTITIBULAR SYSTEM DURING YAW OSCILLATION. NAMRL-1212. Pensacola, FL: Naval Aerospace Medical Research Laboratory, 8 December.

The report describes the results of a system transfer function study of the oculovestitibular response to yaw oscillation. Ten naval aviator candidates were exposed to Earth-vertical rotation about the z head axis at nine different octave-separated frequencies covering the 0.005 to 1.28 Hz spectrum with peak velocity held constant at 50 deg/sec. The frequency dependence of the oculovestitibular system was interpreted in terms of phase and amplitude measures of the resulting horizontal nystagmus. Though the phase data were observed to deviate somewhat from those predicted by the conventional second-order cupula-endolymph model at the lower stimulus frequencies, a theoretical account for the deviation was provided by introducing an adaptation model as developed by other researchers. An adaptation time constant of 100 sec was found to best represent the observed phase response. By taking into account the phase lead introduced by this factor, the lower corner frequency of the cupula-endolymph system was estimated to be 0.0085 Hz (a long time constant of approximately 19 sec).

Aerospace medicine  
Human effectiveness  
Flight forces  
Angular acceleration  
Labyrinth  
Oculovestitibular system  
Semicircular canals  
Cupula-endolymph system  
Eye motions  
Nystagmus  
Biological models  
Frequency response  
Transfer functions  
Bioengineering

Hixson, W. Carroll

1974

FREQUENCY RESPONSE OF THE OCULOVESTITIBULAR SYSTEM DURING YAW OSCILLATION. NAMRL-1212. Pensacola, FL: Naval Aerospace Medical Research Laboratory, 8 December.

The report describes the results of a system transfer function study of the oculovestitibular response to yaw oscillation. Ten naval aviator candidates were exposed to Earth-vertical rotation about the z head axis at nine different octave-separated frequencies covering the 0.005 to 1.28 Hz spectrum with peak velocity held constant at 50 deg/sec. The frequency dependence of the oculovestitibular system was interpreted in terms of phase and amplitude measures of the resulting horizontal nystagmus. Though the phase data were observed to deviate somewhat from those predicted by the conventional second-order cupula-endolymph model at the lower stimulus frequencies, a theoretical account for the deviation was provided by introducing an adaptation model as developed by other researchers. An adaptation time constant of 100 sec was found to best represent the observed phase response. By taking into account the phase lead introduced by this factor, the lower corner frequency of the cupula-endolymph system was estimated to be 0.0085 Hz (a long time constant of approximately 19 sec).

Aerospace medicine  
Human effectiveness  
Flight forces  
Angular acceleration  
Labyrinth  
Oculovestitibular system  
Semicircular canals  
Cupula-endolymph system  
Eye motions  
Nystagmus  
Biological models  
Frequency response  
Transfer functions  
Bioengineering